



1 Regionalization and its impact on global runoff simulations: A 2 case study using the global hydrological model WaterGAP3 3 (v 1.0.0)

4 Jenny Kupzig¹, Nina Kupzig², Martina Flörke¹

5 ¹Institute of Engineering Hydrology and Water Resources Management, Ruhr-University, 44801, Bochum, Ger-
6 many

7 ²Faculty of Management and Economics, Ruhr-University, 44780, Bochum, Germany

8 *Correspondence to:* Jenny Kupzig (jenny.kupzig@rub.de)

9 **Abstract:**

10 Valid simulation results from global hydrological models (GHMs), such as WaterGAP3, are essential to detecting
11 hotspots or studying patterns in climate change impacts. However, the lack of worldwide monitoring data makes
12 it challenging to adapt GHMs' parameters to enable such valid simulations globally. Therefore, regionalization is
13 necessary to estimate parameters in ungauged basins. This study presents new regionalization methods for Wa-
14 terGAP3 and aims to provide insights into selecting a suitable regionalization method and evaluating its impact on
15 the simulation. Our results suggest that machine learning-based methods may be too flexible for regionalizing
16 WaterGAP3 due to a significant performance loss between training and testing. In contrast, the most basic region-
17 alization method (using the concept of spatial proximity) outperforms most of the developed regionalization meth-
18 ods and a pre-defined benchmark-to-beat in an ensemble of split-sample tests. The method selection, whether
19 spatial proximity-based or regression-based, has a greater impact on the regionalization than the specific details
20 on how the method is applied. In particular, the descriptor selection plays a subsidiary role when at least a subset
21 of selected descriptors contains relevant information. Additionally, our research has shown that regionalization
22 causes spatially varying uncertainty for ungauged regions. For example, India and Indonesia are particularly af-
23 fected by higher uncertainty. The impact of regionalization in ungauged areas propagates through the water system,
24 e.g., one water balance component changed by approximately 2400 km³ yr⁻¹ on a global scale, which is in the range
25 of inter-model differences. The magnitude of the impact of regionalization depends on the variability in regional-
26 ized values and the region's sensitivity for the analysed component.

27 **1. Introduction**

28 Global hydrological models (GHMs) are developed and applied worldwide, e.g. to detect hotspots and examine
29 patterns of climate change impacts on the terrestrial water cycle (e.g., Barbarossa et al., 2021; Boulange et al.,
30 2021). Valid model results are a prerequisite to draw robust conclusions. For valid modelling results, it is beneficial
31 to adjust the parameter values to adapt the models to different basin processes (Gupta et al., 1998). This adaptation
32 is usually modified and evaluated (in a loop) by comparing the simulated model output, often discharge, with the
33 monitored data. However, this parameter adjustment for GHMs is challenging due to the lack of global monitoring
34 data. Consequently, parameter adjustment for GHMs can be based not only on monitored data (i.e., calibration)
35 but also on estimating parameter values for ungauged basins (i.e., regionalization).



36 Regionalization is the estimation of parameter values in a model for ungauged basins (Oudin et al., 2008), usually
37 based on information from gauged basins (Oudin et al., 2010). Regionalization methods generally follow the same
38 principle: basin characteristics (e.g., physiographic and/or climatic) are linked to hydrological characteristics and
39 can thus be used to estimate parameter values. Various regionalization methods exist, and no overall preferred
40 method has been found (Ayzel et al., 2017; Pool et al., 2021). In contrast, the optimal regionalization method may
41 differ, for example, regarding available information (Pagliero et al., 2019) or model structures (Golian et al., 2021).
42 Therefore, different methods should be tested to find an optimal regionalization method for a specific use case
43 (e.g., Qi et al., 2020).

44 Evaluation is needed to assess different regionalization methods. Evaluation is particularly challenging for region-
45 alization methods because they are usually applied when monitoring data is missing. Therefore, regionalization
46 studies often treat gauged basins as “ ungauged ” and perform leave-one-out cross-validation (e.g., Chaney et al.,
47 2016) or split-sample tests (e.g., Beck et al., 2016; Nijssen et al., 2000; Yoshida et al., 2022). While at the
48 mesoscale, this evaluation is already an integral part (e.g. McIntyre et al., 2005; Parajka et al., 2005; Oudin et al.,
49 2008; Yang et al., 2020), this is sometimes not the case in global or continental studies (e.g., Müller Schmied et
50 al., 2021; Widén-Nilsson et al., 2007). Another reasonable evaluation strategy is the concept of benchmark-to-beat
51 (Schaefli & Gupta, 2007; Seibert, 2001). Applying a benchmark-to-beat supports a comprehensive evaluation of
52 whether a new approach is functional, e.g., better than a straightforward and thus transparent method or better than
53 a predecessor. To the authors' knowledge, such a benchmark-to-beat has never been used to evaluate innovations
54 in regionalization at the global level.

55 In general, regionalization methods can be divided into two categories based on the parameter estimation strategy:
56 (1) regression-based and (2) distance-based (He et al., 2011). Regression-based methods derive the relationship
57 between basin characteristics and model parameters through fitted regression models. These mathematically de-
58 fined relationships are further applied to estimate model parameters of ungauged basins (e.g. Kaspar, 2004; Müller
59 Schmied et al., 2021). A significant drawback of regression-based regionalization is the difficulty of incorporating
60 parameter interdependencies (Poissant et al., 2017). Regression-based approaches often assume that the dependent
61 variables, i.e., the model parameters, are not correlated (Wagener et al., 2004). Distance-based approaches transfer
62 complete parameter sets from similar or nearby donor basins to ungauged basins (e.g., Beck et al., 2016; Nijssen
63 et al., 2000; Widén-Nilsson et al., 2007). Using an ensemble of donor basins, e.g., by averaging the parameter
64 values or model outputs, can improve the performance of such methods (e.g., Arsenault & Brissette, 2014). A
65 significant disadvantage of such methods is the clustering problem of ungauged basins, i.e., the unequal distribu-
66 tion of gauging stations worldwide (Krabbenhoft et al., 2022). Thus, basins exist where distance-based approaches
67 will use incomparable basins to transfer parameter values due to the lack of close basins.

68 Recent advances have implemented machine learning-based techniques in the context of regionalization. For ex-
69 ample, Chaney et al. (2016) used regression trees as an alternative to least squares regression to estimate parameter
70 values in ungauged basins. Pagliero et al. (2019) explored supervised and unsupervised clustering methods to
71 define the similarity of basins to transfer parameter sets. To the authors' knowledge, no study has compared several
72 traditional regionalization methods with machine learning-based methods for a GHM on a global scale.

73 Some regionalization methods do not make a clear distinction between calibration and regionalization. For exam-
74 ple, Arheimer et al. (2020) applied a basin grouping beforehand. Then, they jointly calibrated the group members
75 to define representative parameter sets. Subsequently, the representative parameter sets are transferred to other



76 basins based on grouping rules. Another approach defines so-called transfer functions (Samaniego et al., 2010)
77 and calibrates meta-parameters instead of the model parameter values (Beck et al., 2020; Feigl et al., 2022). These
78 methods, where regionalization is part of the calibration process, often require a change in the calibration process
79 itself, which is challenging for GHMs (Schweppe et al., 2022), for example, due to a lack of code flexibility (e.g.,
80 Cuntz et al., 2016).

81 This study proposes an improved regionalization method for the state-of-the-art GHM WaterGAP3 (Eisner, 2016).
82 It compares traditional regionalization methods with machine learning-based methods and uses a “benchmark-to-
83 beat” and an ensemble split-sample test to evaluate the applied methods. The overall research topic is evaluating
84 and selecting the most appropriate regionalization method for a GHM. Specifically, the study has two objectives.
85 It aims

- 86 (1) to propose a selection for the regionalization method of WaterGAP3 and
- 87 (2) to evaluate the impact of an improved regionalization method against a benchmark-to-beat.

88 2. Data and Methods

89 2.1 The Model: WaterGAP3

90 The GHM WaterGAP3 simulates the terrestrial water cycle, including the main water storage components and a
91 simple storage-based routing algorithm. It is a fully distributed model that operates on a five arcmin grid and
92 simulates at a daily time step. A more detailed model description can be found in Eisner (2016).

93 In WaterGAP3, most model parameter values are set a priori, e.g., using look-up tables for albedo or rooting depth.
94 Only one parameter, γ , is calibrated, which is part of the soil moisture storage in which runoff generation processes
95 are present. The model equation for γ , which originates from the HBV-96 model (Lindström et al., 1997), is given
96 in Eq. (1). Generally, higher values of γ lead to lower runoff volumes, while lower values of γ lead to higher runoff
97 volumes. This model parameter is calibrated per basin within the range of 0.1 and 5. The objective function for
98 calibration is to minimize the deviation between the mean annual simulated and observed river discharge. Thus,
99 as a result of the calibration, each basin has a calibrated value (γ) between 0.1 and 5. After the calibration, a
100 correction is applied to account for high errors in the mass balance, e.g., due to inaccuracies in global meteorolog-
101 ical forcing products. This correction can only be applied in gauged basins. It is, therefore, neglected in this study.

$$102 \quad R = P_t \cdot \left(\frac{S_s}{S_{s,max}} \right)^\gamma \quad (1)$$

103 where R is the daily runoff, P_t is the daily throughfall, S_s is the actual soil storage, $S_{s,max}$ is the maximal soil
104 storage, and γ is the calibration parameter.

105 Traditionally, the regionalization process in WaterGAP3 is a simple multiple linear regression (MLR) approach to
106 estimate the calibration parameter γ for ungauged basins (e.g., Döll et al., 2003; Kaspar, 2004). The drawback of
107 MLR regarding parameter interaction can be neglected: As there is only one parameter to estimate, parameter
108 interference does not exist. Instead, the approach offers the advantage of a lightweight, transparent application that
109 can be quickly revised and adapted. We use the regionalization approach from WaterGAP2.2d as benchmark-to-
110 beat as defined in Müller Schmied et al. (2021). WaterGAP2 has a model structure and calibration process that are



111 very similar to WaterGAP3. The main difference between these models is that WaterGAP2.2d simulates at
112 0.5°spatial resolution. Thus, we expect the regionalization approach to be feasible for WaterGAP3.

113 2.2 Model Data

114 WaterGAP3 requires various input data, such as soil information, topography, or information on open freshwater
115 bodies. This study uses the same input data as Kupzig et al. (2023). For meteorological forcing, we use the global
116 data set EWEMBI (Lange, 2019). This data product includes daily global forcing data with a spatial resolution of
117 0.5 degrees (latitude and longitude) that covers a period from 1979 to 2016. Specifically, WaterGAP3 uses the
118 following forcing information from the EWEMBI data set as input:

- 119 • daily mean temperature,
- 120 • daily precipitation,
- 121 • daily shortwave downward radiation, and
- 122 • daily longwave downward radiation.

123

124 The WaterGAP3 calibration requires observed monthly river discharge data. This discharge data is subsequently
125 transformed into annual discharge sums in the calibration procedure and used as a benchmark. In this study, we
126 used discharge data from 1,861 stations that were manually verified (Eisner, 2016). To get the best data available,
127 we have updated all available station data with recent data from The Global Runoff Data Center (GRDC). All
128 stations have at least five years of complete (monthly) station data between 1979 and 2016. For each station, a
129 contribution area, i.e., a basin, is defined with the gridded flow-direction information obtained from WaterGAP3,
130 which is based on the HydroSHEDS database (Lehner et al., 2008).

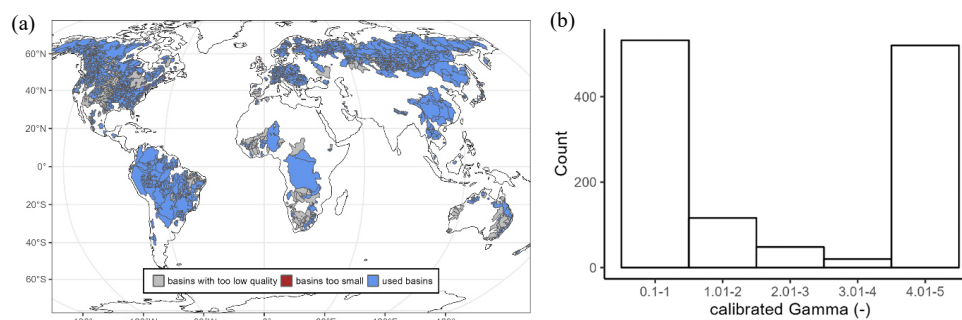
131 The 1,861 basins are calibrated using the standard calibration approach for WaterGAP3. After the standard cali-
132 bration, some basins still have an insufficient model performance, i.e., more than 20% bias in monthly discharge.
133 These basins are neglected in further analysis to avoid high parameter uncertainty due to errors in input data, model
134 structure, or discharge data affecting the analysis. Further, we have excluded all basins with less than 5000 km²
135 (inter-) basin size to the next upstream basin. We assume that this inter-basin size is large enough to assume a
136 certain degree of interdependency between nested basins. In total, 1,236 basins out of 1,861 basins are selected for
137 regionalization (323 are neglected due to low model performance, and 302 are neglected due to insufficient basin
138 size).

139 Figure 1a shows a map of the worldwide calibrated basins, covering most parts of North and South America.
140 However, Africa and Oceania remain largely ungauged. A cluster of gauged basins is located in Central Europe
141 and Eastern Asia. Gauged regions with low model performance are mainly found in the Mississippi River basin,
142 Southern Africa and Australia. These regions are known to be challenging for GHMs (e.g., cf. Fig. 8b in Stacke &
143 Hagemann, 2021).

144 Figure 1b shows the calibrated values for γ . It emerges that the calibrated values tend to bet at the upper and lower
145 bounds of the parameter space. This misbehaviour is already known (cf. Fig. 4b in Müller Schmied et al., 2021)
146 and highlights the need to further develop the calibration strategy for WaterGAP3, e.g., by implementing multi-
147 variate calibration. However, this study focuses solely on analysing and implementing a new regionalization
148 method. It does not aim to change the calibration approach of WaterGAP3. To achieve the latter, future studies are



149 needed to select sensitive parameters or advance the model structure to avoid structural errors that introduce high
150 parameter uncertainty when applying multivariate calibration (Kupzig et al., 2023).



151 **Figure 1: (a) Gauged basins calibrated beforehand, highlighting basins not used for regionalization due to low model**
152 **performance or too small basin size and (b) the histogram of the calibrated model parameter values of all used basins**
153 **showing heavy-tails.**

154 2.3 Basin Descriptors

155 This study uses basin descriptors as predictors to drive regression-based or distance-based regionalization ap-
156 proaches. These basin descriptors are based on model data and are aggregated to basin values using a simple mean
157 method to have the exact spatial resolution as the calibrated model parameter. Thus, in the case of nested basins,
158 the inter-basin area is used to define the basin descriptors. The selection of the predictors, i.e., basin descriptors
159 that support the estimation of γ , is crucial for regionalization methods (Arsenault & Brissette, 2014). Typically,
160 this selection aims to obtain the most information with the least number of predictors to (1) improve the model
161 quality and (2) limit over-parametrization. In this study, we use 12 basin descriptors to develop regionalization
162 methods; nine of these descriptors are physiographic, while the remaining three are climatic (see Table 1). Most
163 descriptors are not correlated (see Appendix A), i.e., we avoid redundant information (Wagener et al., 2004).

164 The predictor selection is based on correlation analysis and entropy assessment. Pearson's correlation coefficient
165 detects linear correlation, and Spearman's Rho and Kendall's Tau detect a non-linear correlation between basin
166 descriptors and calibrated γ values. Shannon entropy (Shannon, 1948) measures the information gain of the pre-
167 dictors explaining the calibrated γ value. The higher the information gain, the more valuable the basin descriptor
168 is for explaining the variation in the calibrated γ value.

169 The correlation coefficients and the corresponding information gain are listed in Table 1. All basin descriptors
170 have a low correlation coefficient, e.g., the highest Pearson correlation is -0.36. The information gain shows the
171 same result for the predictors, i.e., descriptors with a higher correlation tend to have a higher information gain.
172 Nevertheless, the information gain is relatively low, with a maximum of 14.4% of the information explained by
173 the temperature descriptor. A possible reason for the low correlation and information gain is that the γ values are
174 tailored within the calibration's valid parameter bounds (i.e., 0.1 and 5), resulting in heavy tails of the calibrated γ
175 distribution. Thus, we expect the correlation to be higher, with calibrated γ reaching values higher than 5. In addi-
176 tion, the calibrated value masks the effect of multiple sources of errors, such as uncertainty in the input data, model
177 structure, or varying hydrological processes. Thus, there might be more complex relationships between the de-
178 scriptors and the calibrated parameter, which are only partially captured by this analysis. Nevertheless, the results
179 of this analysis indicate descriptors that may be more useful than others in defining a regionalization method. We



180 implement regionalization methods using four groups of basin descriptors by selecting basin descriptors with the
 181 highest correlation coefficients and information gain:

- 182 • “cl”: two correlated climatic descriptors (mean temperature, annual shortwave radiation),
- 183 • “p”: three correlated physiographic descriptors (slope class, forest %, permafrost %),
- 184 • “p+cl”: two correlated climatic & three physiographic descriptors, and
- 185 • “all”: all 12 descriptors (as a control group to examine the effect of using correlated descriptors).

186

187 **Table 1: Basin descriptors used in the regionalization methods: statistical information, correlation, and entropy assess-**
 188 **ment. Selected physiographic and climatic basin descriptors are shaded in grey.**

	Basin Descriptor	Attribute Information				Entropy & Correlation			
		Min	Max	Mean	Median	IG (%)	Pearson	Spearman	Kendall
physiographic	Soil Storage (mm)	8.994	677.950	219.071	192.006	10.19	-0.20	-0.16	-0.12
	Open Water Bodies (%)	0.000	77.125	7.979	2.376	5.22	0.01	-0.05	-0.03
	Wetlands (%)	0.000	73.181	6.134	0.721	4.60	0.02	-0.07	-0.05
	Size (km ²)	5000	3112480	36811	13850	1.08	-0.03	-0.01	-0.01
	Slope Class (-)	10.057	67.756	37.739	36.986	14.22	-0.27	-0.31	-0.23
	Altitude (m.a.s.l.)	22.324	4765.166	630.826	412.414	7.29	-0.11	-0.19	-0.14
	Sealed Area (%)	0.000	12.3	0.5	0	3.25	0.18	0.34	0.25
	Forest (%)	0.000	100.000	32.037	18.245	11.50	-0.27	-0.21	-0.16
	Permafrost & Glacier (%)	0.000	95.000	15.316	0.000	10.96	-0.36	-0.47	-0.37
climate	Mean Temperature(°C)	-18.848	28.998	7.769	6.562	14.36	0.34	0.39	0.29
	Yearly Precipitation (mm)	73.1	5716.3	950.6	743.5	7.95	0.01	0.18	0.13
	Yearly Shortwave Downward Radiation (Wm ⁻²)	1050.6	33098.4	1887.5	1777.2	13.05	0.33	0.34	0.25

189

190 2.4 Regionalization Methods

191 In our study, we test several traditional and machine learning-based regionalization methods against each other
 192 and a defined benchmark-to-beat to find the most suitable regionalization method for WaterGAP3. At the global
 193 scale, regionalization is particularly challenging due to (1) the lack of high-quality data, (2) the diversity of dom-
 194 inant hydrological processes in basins and (3) the high computational demands of the models. Therefore, a region-
 195 alization method that is robust, applicable to a wide variety of basins, and not computationally demanding should
 196 be chosen.

197 We test three common traditional approaches: spatial proximity, physical similarity, and regression-based meth-
 198 ods, as well as two machine learning-based approaches. These machine learning-based approaches are alternatives
 199 to traditional physical similarity and regression-based methods. As the model calibration of WaterGAP3 is very
 200 rigid and has only one parameter, it is not feasible to implement and test regionalization methods that incorporate
 201 regionalization into the calibration process, such as transfer functions. In addition, we avoid high computational
 202 demands as all methods can be applied after the calibration, i.e., without running the model.

203 To evaluate the regionalization methods, we implement an ensemble of split-sample tests. Specifically, we ran-
 204 domly split the basins into 50% gauged and 50% pseudo-ungauged basins. This split has a relatively high percent-
 205 age of pseudo-ungauged basins, accounting for many missing gauges worldwide. We fit the methods and apply
 206 them to the training and testing data sets. The split-sample test is repeated 100 times with randomly selected basins
 207 for training and testing to account for sampling effects.



208 As there is only one calibration parameter, γ , this parameter has a global optimum per basin. Consequently, the
209 quality of training and testing is directly assessed by the deviation between the predicted and calibrated γ . Thus,
210 the mean absolute error (MAE), an easy-to-interpret measure, is used to evaluate the prediction accuracy. The
211 lower the MAE, the better the prediction; an MAE of zero expresses no error. In our case, an MAE of 2.1 corre-
212 sponds to the error when using the mean calibrated γ value as the predicted value. The regionalization method is
213 robust if the prediction accuracy is similar in training and testing. A generally good performance, i.e., small MAE
214 values, indicates that the regionalization method suits WaterGAP3.

215 **Regression-based methods**

216 For the traditional regression-based methods, we use the `lm()` function of the R package `stats` (R Core Team, 2020)
217 to implement an MLR. After applying the regression model, we adjust the estimated parameter values to ensure
218 that the estimated values range between 0.1 and 5. As the calibration of WaterGAP3 results in a parameter distri-
219 bution with heavy tails, we implement a so-called “tuning approach” to introduce this information into regionali-
220 zation. In detail, we apply a simple threshold-based approach to adjust the regionalized parameter values to the
221 extremes, i.e., $\gamma_{est} < \gamma_1 \rightarrow \gamma_{reg} = 0.1$ and $\gamma_{est} > \gamma_2 \rightarrow \gamma_{reg} = 5.0$. A simple clustering, i.e., the k-means algo-
222 rithm with three centres, defines these thresholds.

223 Furthermore, a machine learning-based method, namely random forest (RF), is tested for regionalization. Here,
224 we implement the random forest algorithm with the `randomForest()` function from the R package `randomForest`
225 (Liam & Wiener, 2002), which is based on Breimann (2001). The algorithm uses an ensemble of decision trees,
226 making the decision human-like. It is relatively robust because it incorporates random effects into the training
227 process. To implement this randomness, we define that the algorithm can choose between two randomly selected
228 predictors at each node. We use an ensemble of 200 trees, the same combinations of predictors and the same tuning
229 as for MLR.

230 The benchmark-to-beat defined in Müller Schmied et al. (2021) also uses an MLR approach. This MLR approach
231 relates the natural logarithm of γ to the following basin descriptors: mean temperature, mean available soil water
232 capacity, fraction of open freshwater bodies, mean slope, mean fraction of permafrost coverage and an aquifer-
233 related groundwater recharge factor. Thus, the main differences between the benchmark-to-beat and our defined
234 MLR-based approach are the natural logarithm, our proposed tuning procedure for the method itself, and using the
235 aquifer-related groundwater recharge factor as a basin descriptor.

236 **Physical Similarity**

237 For a traditional physical similarity approach, we use Similarity Indices (in the following named with SI). We use
238 the methodology proposed by Beck et al. (2016). The SI (see Eq. (2)) are derived using the basin descriptors
239 mentioned above, and the parameter of the most similar basin is transferred to the pseudo-ungauged basin. Addi-
240 tionally, we use an ensemble of basins to control whether an ensemble-based approach leads to more robust results.
241 The optimal number of donor basins may vary between research regions and hydrological models (Guo et al.,
242 2020). Here, we use ten donor catchments (noted with “10”), which is based on Beck et al. (2016) and McIntyre
243 et al. (2006). Further, we apply a simple mean method for the ensemble-based prediction to aggregate the ensemble
244 values into one predicted parameter value.



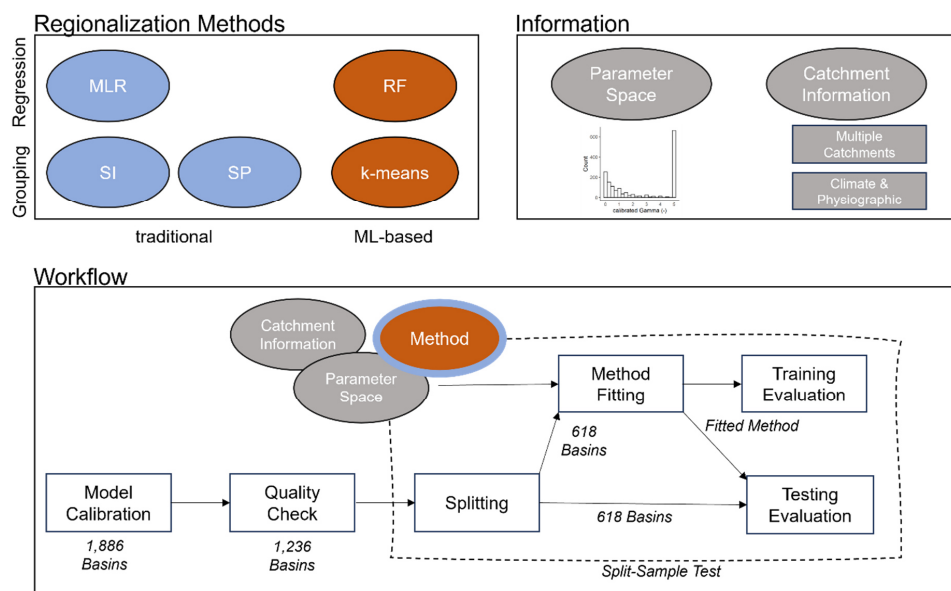
245
$$S_{i,j} = \sum_{p=1}^n \frac{|Z_{p,i} - Z_{p,j}|}{IQR_p} \quad (2)$$

246 where $S_{i,j}$ is the Similarity Index between basin i and basin j , $Z_{p,j}$ is the basin descriptor p for basin j , IQR_p is the
 247 interquartile range for basin descriptor p among all (gauged) basins, and n is the number of all basin descriptors
 248 used.

249 As a machine learning-based approach, we apply a simple k-means algorithm. We selected the k-means algorithm
 250 because it is one of the most widely used clustering algorithms (Tongal & Sivakumar, 2017). It is easy to under-
 251 stand and use. The algorithm `kmeans()` is implemented in the R base package `stats`. It aims to maximize variation
 252 between groups and minimize variation within groups. We use three clusters to generate the groups of basins. As
 253 different scales of the predictor values can affect the clustering, a rescaling with min-max-normalization (see Eq.
 254 (3)) is performed on the training set and applied to the testing set. After the grouping, the mean γ value is assigned
 255 as a representative calibrated value to the corresponding basin group. To estimate the corresponding group for a
 256 pseudo-ungauged basin, the knn algorithm is used and the representative γ value of the group is assigned to the
 257 pseudo-ungauged basin. This algorithm is implemented by the `knn()` function of the R package class (Venables &
 258 Ripley, 2002). Since this method is less flexible than SI, we implement a highly flexible version of k-means with
 259 162 groups, where each ungauged basin is sorted into a very small basin group. Using this highly flexible version
 260 of k-means, we test whether the potential differences between SI and k-means are based on the degree of flexibility.

261
$$Z'_{p,j} = \frac{Z_{p,j} - \min_{j \rightarrow m}(Z_{p,j})}{\max_{j \rightarrow m}(Z_{p,j}) - \min_{j \rightarrow m}(Z_{p,j})} \quad (3)$$

262 where $Z'_{p,j}$ is the normalised basin descriptor p for basin j , $Z_{p,j}$ is the basin descriptor p for the basin j , m is the
 263 number of (gauged) basins.



264
 265 **Figure 2: Experimental setup of the study: regionalization methods, used modifications and information and the general**
 266 **workflow (MLR: Multiple Linear Regression, SI: Similarity Indices, SP: Spatial Proximity, RF: RandomForest).**



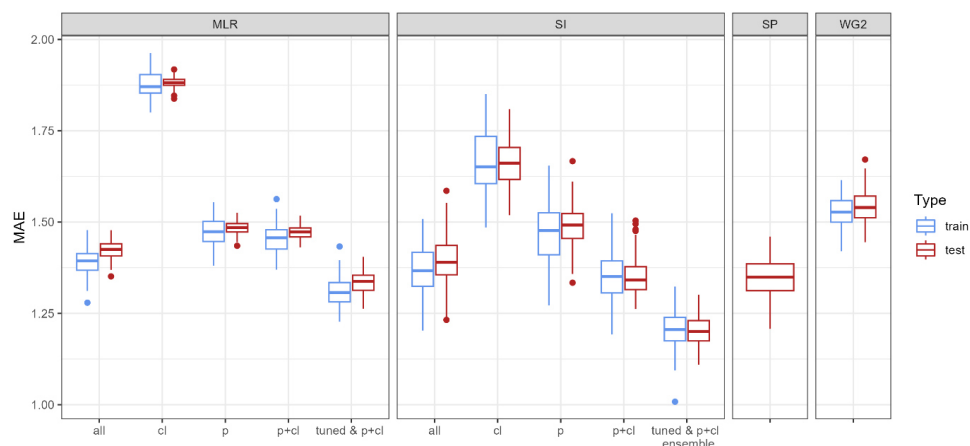
267 Spatial Proximity

268 The spatial proximity approach is one of the easiest to regionalize parameter values. However, it is also often
269 criticized that nearby basins do not necessarily have the same hydrological behaviour (Wagener et al., 2004).
270 Furthermore, its performance depends on the density of the network of gauged basins (Lebecherel et al., 2016).
271 The dependency on network density is particularly challenging for global applications where large parts of the
272 world are ungauged (e.g., northern Africa). Nevertheless, the approach has been successfully applied in other
273 studies (e.g., Oudin et al., 2008; Qi et al., 2020), even globally (Widén-Nilsson et al., 2007). Here, we take the
274 distance between the centroids of the basins as a reference for the spatial distance between basins, as done by
275 others (Oudin et al., 2008). We use the abbreviation SP in the text below to refer to the spatial proximity approach.
276 Figure 2 provides an overview of the applied regionalization methods and information used for the experimental
277 setup.

278 3. Results and Discussion

279 3.1 Evaluating Traditional Methods

280 Here, we examine the traditional methods (MLR, SI, SP) by comparing the ensemble of MAEs from training and
281 testing to each other and the benchmark-to-beat (see Fig. 3). As for all traditional methods, there is no significant
282 performance loss between training and testing, we will further focus on the performance in testing for evaluating
283 the methods. When assessing the MLR and the SI approach, it becomes apparent that using only the climatic
284 descriptors is insufficient for regionalization as it provides worse estimates than the benchmark-to-beat. The ex-
285 clusive selection of physiographic descriptors (slope class, forest %, and permafrost %) performs better, and yields
286 results comparable to our benchmark-to-beat for both methods. Using climatic and physiographic descriptors
287 jointly increases the performance of SI by approximately 0.1 in median MAE. For MLR, the improvement is
288 almost neglectable.



289

290 **Figure 3: Split-sampling results for the benchmark-to-beat taken from WaterGAP2 (WG2) and different versions of**
291 **the traditional regionalization methods: Multiple Linear Regression (MLR), Similarity Indices (SI) and Spatial Prox-**
292 **imity (SP).**



293 Thus, using only climatic descriptors - in our case, the mean temperature and information about radiation - is
294 insufficient for regionalization. Instead, physiographic descriptors appear more critical for regionalization than the
295 selected climatic descriptors. However, the best results are obtained when combining climatic and physiographic
296 descriptors. Others often apply the combination of climatic and physiographic descriptors, leading to optimal re-
297 gionalization results (e.g., Oudin et al., 2008; Reichl et al., 2009).

298 The reduced importance of climatic descriptors is surprising, as the climatic descriptors tend to have a higher
299 information gain and correlation to the model parameter (see Table 1). Moreover, climatic information is often
300 used as a central part of other regionalization studies, e.g., to assess regionalization (e.g., Parajka et al., 2013; Guo
301 et al., 2020). One possible reason for this discrepancy in other studies is that we used pure meteorological data as
302 climatic descriptors for the regionalization method. In contrast, others used derived information such as Köppen-
303 Geiger climate zones or the Aridity Index (e.g., Beck et al., 2016; Yoshida et al., 2022).

304 When expanding the analysis to all descriptors, the performance changes slightly (i.e., mean MAE +/- ~0.05).
305 Thus, increasing the number of descriptors does not increase the performance of regionalization at some point (in
306 line with Oudin et al., 2008 using a comparable Physical Similarity approach). This suggests that uncorrelated,
307 non-redundant descriptors do not interfere with the regionalization using SI and MLR. Instead, a certain amount
308 of information is beneficial to increase the regionalization method. After reaching this point, adding descriptors
309 does not increase the performance, probably because all extractable information is already present in the given
310 descriptors.

311 Using an ensemble of ten donor basins for the SI approach results in slightly better MAE values in most cases than
312 applying a single donor basin (see Appendix B). More remarkably, the variation in the MAE values decreases
313 significantly for all ensemble approaches (i.e., the reduction in standard deviation in MAEs is about 50%). Thus,
314 introducing an ensemble approach for SI does not significantly improve the prediction performance. Still, it in-
315 creases the likelihood that the prediction will perform well, i.e., be more robust. The positive effect of an ensemble
316 approach for SI is already noted (Oudin et al., 2008). However, the literature-based number of donor basins might
317 be adopted in future applications to be optimal for WaterGAP3, probably leading to higher performance.

318 The introduction of tuning led to a significant increase in prediction performance for MLR, i.e., the median MAE
319 for all MLR approaches improved by 0.04 (“cl”) and ~0.14 (others). For the ensemble-based SI approach, the
320 tuning improves the median MAE by about 0.07 to 0.12. Thus, applying knowledge of the optimal parameter space
321 enhances the quality of regionalization. This positive effect is not surprising, as incorporating a-priori information
322 about parameter distribution strengthens parameter estimation (e.g., described in Tang et al., 2016 using the Bayes
323 Theorem).

324 The SP approach is the simplest applied, evaluating distances to the centroids without requiring regression or
325 clustering. Thus, there is no training performance, only a testing performance. Applying the approach leads to a
326 median MAE of 1.356, which is better than the benchmark-to-beat (median MAE in the testing of 1.544) and has
327 the same quality as the best MLR and SI approaches without tuning (median MAE of 1.394 and 1.367, respec-
328 tively). The good performance of SP is in accordance with other studies (e.g., Oudin et al., 2008; Qi et al., 2020).
329 It indicates that this simple approach is suitable for WaterGAP3.

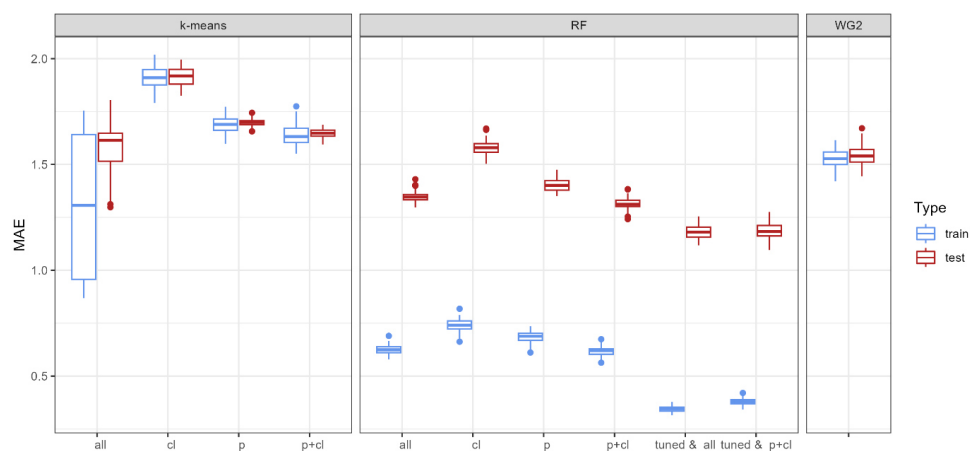
330 Nevertheless, the well-performing SP on a global scale is surprising as the distances between basins are potentially
331 large and hydrological processes may strongly vary. It is probably beneficial for the SP approach that γ comprises



332 all kinds of errors, e.g., spatially localised errors in global forcing products (e.g., Beck et al., 2017 reported errors
333 for arid regions in the precipitation product) or inaccurately represented processes for larger regions. Thus, the
334 estimation of γ might be appropriate, but not because of the same hydrological behaviour but due to the same kind
335 of errors.

336 3.2 Evaluating Machine Learning-based Approaches

337 In this section, we assess whether machine learning-based approaches outperform the benchmark-to-beat and are
338 suitable as a new regionalization method for WaterGAP3. We compare the ensemble of MAE for training and
339 testing for RF and k-means with the benchmark-to-beat (see Fig. 4).



340
341 **Figure 4: Split-sampling results for the benchmark-to-beat taken from WaterGAP2 (WG2) and different versions of**
342 **machine learning-based approaches: k-means (in combination with knn) and RandomForest (RF).**

343 The RF approach is highly accurate within the training, i.e., fitting to calibrated γ values works well for gauged
344 basins. However, it suffers a significant loss in performance when predicting the γ values for the pseudo-ungauged
345 basins. Although RF still has low MAE values in testing, the loss in performance from training to testing is signif-
346 icantly higher compared to other methods. This performance loss indicates that RF is not a robust regionalization
347 method for WaterGAP3. Other studies which reported good performance of RF in terms of regionalization have
348 not investigated the stability of the performance from training to testing (Golian et al., 2021; Wu et al., 2023).
349 Likely, the mathematical problem of predicting the calibrated parameter for WaterGAP3, with all its challenges
350 (e.g., tailored and heavy-tailed parameter space, incorporation of many sources of errors), cannot be adequately
351 solved by RF. Thus, although RF is known to be especially robust among other machine learning-based techniques,
352 it shows symptoms of over-parameterization, meaning that the algorithm is too flexible and adjusts to noise in the
353 data, missing the underlying systematic. This lack of robustness is particularly disadvantageous since, for Wa-
354 terGAP3, regionalization is applied globally, requiring regionalizing large parts of the world.

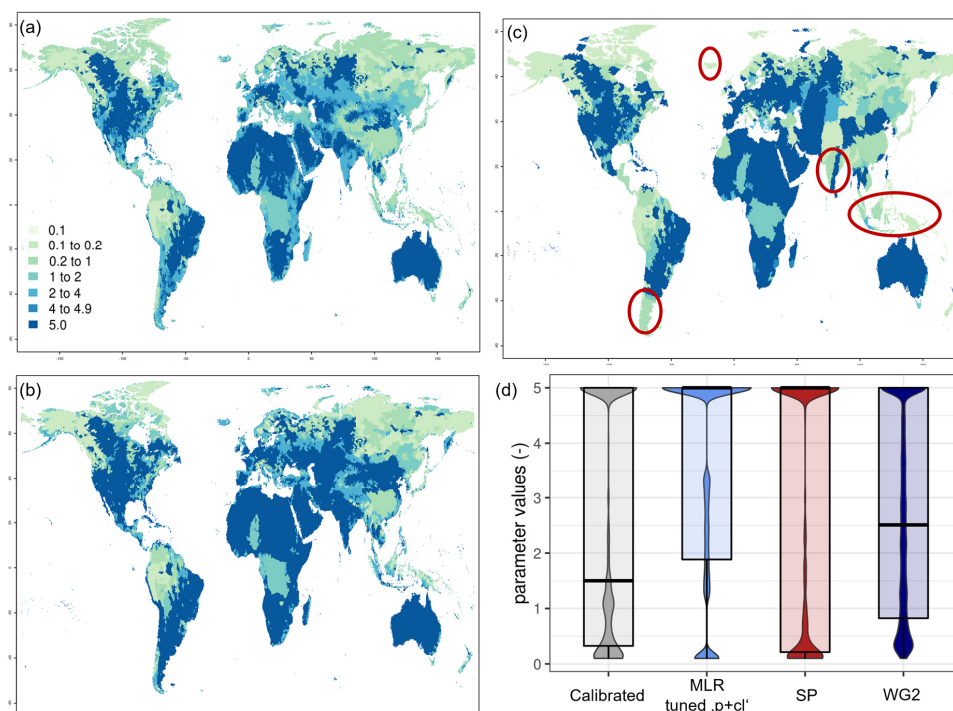
355 The k-means approach does not show such a performance loss between training and testing in almost all variants.
356 The only variant with comparable performance loss is the “highly flexible” k-means approach. Interestingly, the
357 “highly flexible” k-means approach was developed to emulate the same flexibility as in SI, which does not show
358 such performance loss between training and testing. This difference in robustness indicates that the applied k-
359 means algorithm does not extract the information from the descriptors as efficiently as the SI approach. The lack



360 of efficient data use for some clustering methods in the context of regionalization has already been reported by
361 Pagliero et al. (2019). This could also contribute to the presented the k-means falling behind the benchmark-to-
362 beat. Therefore, we conclude that the developed clustering is inappropriate for regionalizing WaterGAP3.

363 3.3 Implications of Regionalization

364 Finally, we highlight the possible implications of choosing regionalization methods for GHMs, where large parts
365 of the world need to be regionalized. For this purpose, a local analysis of internal states and fluxes and a continental
366 and global assessment of the water balance are undertaken. Therefore, we run WaterGAP3 from 1980 to 2016 with
367 different γ distributions. We choose two equally valid solutions for the regionalization of WaterGAP3 to produce
368 equally valid global γ distributions: (1) the SP approach because of its simplicity and because it outperforms our
369 benchmark-to-beat, and (2) the tuned MLR “p+cl” because it outperforms our benchmark-to-beat and its applica-
370 tion is very similar to the original regionalization approach of WaterGAP3. The tuned Similarity Indices “p+cl”
371 with an ensemble of 10 donor basins is also a valid solution for regionalizing γ . However, its application is more
372 complex than MLR and SP and differs considerably from the original WaterGAP3 regionalization. Therefore, it
373 has not been implemented and tested. In addition, we run the model with our benchmark-to-beat as it is our refer-
374 ence for assessing changes. We use the best-performing benchmark-to-beat and MLR models out of the 100 trained
375 models for the analysis.

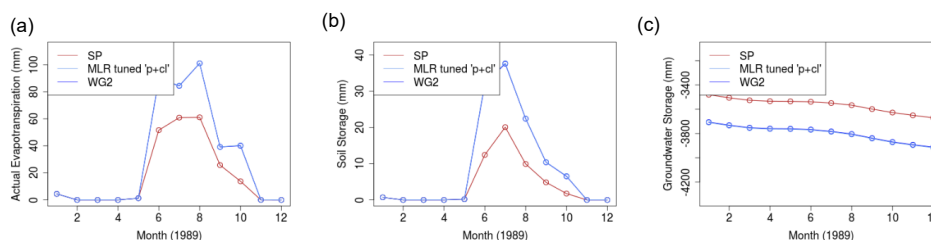


376

377 **Figure 5: Global γ distribution for different regionalization methods, highlighting areas of differences (a) γ distribution**
378 **using the MLR approach with parameter space tuning, using physiographic and climatic basin descriptors as independ-**
379 **ent variables, i.e., tuned MLR “p+cl”, (b) benchmark-to-beat, WG2, (c) Spatial Proximity approach, i.e., SP and (d)**
380 **global distribution of regionalized and calibrated parameter values.**

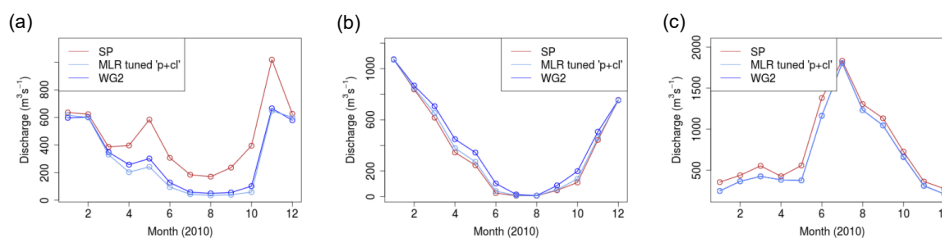


381 First, we compare the resulting global distribution of γ values for all three approaches (see Fig. 5). In particular,
 382 ungauged regions such as Indonesia, India and New Zealand exhibit significant differences in the predicted γ value.
 383 For these regions, the regionalized value varies depending on the methods used for regionalization. In contrast,
 384 ungauged areas such as North Africa do not differ much in regionalized values. Regionalization, therefore, appears
 385 to lead to a spatially varying uncertainty in ungauged regions. The differences in the regionalization methods also
 386 become apparent when comparing the resulting distribution of γ (see Fig. 5d). The approach MLR tuned “p+cl”
 387 tends to predict values at the upper bound more often than the other methods, which is probably due to the tuning
 388 within the method. The benchmark-to-beat approach from WaterGAP2 leads to a less heavy-tailed prediction than
 389 others. The SP-based approach shows the highest similarity to the distribution of the calibrated γ values.



390 **Figure 6: Differences in monthly internal states and fluxes of WaterGAP3 for one grid cell with varying regionalized**
 391 **value (SP: 0.325, MLR tuned “p+cl”: 5 and benchmark-to-beat (WG2): 4.467243), located in India**
 392 **(21.519794°|70.566733°) for a) actual evapotranspiration, b) soil storage and c) groundwater storage for 1989 as an**
 393 **exemplary year. Note that MLR tuned “p+cl” and WG2 are so close that they appear to be one line.**

394 To highlight the impact of local differences in the parameter value, we examine an exemplary location in India
 395 where the regionalized values are 0.325, 5 and 4.467243 for SP, MLR tuned “p+cl” and the benchmark-to-beat,
 396 respectively. We show the resulting actual evapotranspiration (AET), the filling of the soil storage and the ground-
 397 water storage for one exemplary year (see Fig. 6). The internal states and fluxes from the MLR tuned “p+cl” and
 398 the benchmark-to-beat are not significantly different for all states, as the two lines are very close and appear to be
 399 one single line. However, there are considerable differences between the two MLR-based approaches and SP,
 400 particularly in the amplitude of the AET and the soil storage. Acceleration effects cause the lower amplitudes for
 401 these two components. Reducing values of γ leads to a faster outflow of the soil storage, resulting in lower AET
 402 and soil moisture; additionally, smaller values of γ lead to higher groundwater storage due to accelerated percola-
 403 tion.



404 **Figure 7: Simulated monthly runoff using three different regionalization methods for a) the Tiber, b) the Ebro and c)**
 405 **Rio Negro (in Argentina) for 2010 as an exemplary year.**

406 Further on, we highlight the local effects of regionalization on discharge for the Tiber, the Ebro and Rio Negro for
 407 one exemplary year in Figure 7. Whereas the simulated discharge is higher for SP compared to the other methods



408 in the Tiber and Rio Negro, the discharge is lower for the Ebro. Thus, one regionalization method does not always
409 increase or decrease the discharge but results in locally varying effects on the water balance. Moreover, the similar
410 results for MLR tuned “p+cl” and the benchmark-to-beat on the grid cell level (see Figure 6) propagate to a similar
411 discharge pattern at the basin scale. Further, differences between SP and the other regionalization methods at the
412 grid scale can lead to high differences at the basin scale, i.e., the simulated discharge of the Tiber is almost doubled
413 for SP in May.

414 Finally, we evaluate how the observed variation due to different regionalization approaches propagates globally.
415 Therefore, we assess the quantitative influence of regionalization by comparing a key component of the water
416 balance, i.e., outflow to the ocean and inland sinks. Table 2 shows the resulting differences in the selected flow
417 for all three model runs, aggregated to continental and global scales. The results highlight that the differences in
418 mean annual outflow vary spatially and between the regionalization methods. The results of SP differ significantly
419 from the two MLR-based approaches in some parts of the world. In Oceania, the SP approach exhibits a deviation
420 of 7.7 % in the selected flow compared to the benchmark-to-beat. This difference may be attributed to the signifi-
421 cant disparity in γ between the two methods in New Zealand (see Fig. 5).

422

423 **Table 2: Mean outflow to the ocean and inland sinks in $\text{km}^3 \text{yr}^{-1}$ between 1980-2010**

Continent	benchmark-to-beat	MLR	SP
Africa	5005.10	0.972	0.968
Asia	15977.39	1.005	1.114
Oceania	1188.42	0.977	0.923
Europe	3028.47	0.981	1.030
South America	11612.39	0.997	1.039
North America	7283.21	0.994	1.025
Global	44094.97	43876.01	46456.35

424

425 Similarly, SP exhibits a high deviation of 11.4 % in the mean outflow in Asia, which is likely due to the variation
426 of γ in India (see Fig. 5). In contrast, the southern part of South America, which shows a relatively high deviation
427 in γ , does not lead to a significant deviation in the mean outflow for the continent. This limited impact of varying
428 parameter values in southern South America may be attributed to the lower water availability in this region, which
429 only slightly affects the continental water balance. These results suggest that the impact of regionalization methods
430 on the continental water balance depends on (1) the variation in predicted parameter values and (2) the region's
431 sensitivity to the water balance. Examining the global estimates, the differences between the benchmark-to-beat
432 and SP results in approximately $2400 \text{ km}^3 \text{yr}^{-1}$ which is in the range of inter-model differences (see Table 2 in
433 Widen-Nilsson et al.,2007).

434 Although the two newly developed methods performed similarly during the split-sample test, significant differ-
435 ences were observed when simulating the water balance. It was expected that the methods MLR tuned “p+cl” and
436 SP methods would differ less due to their similar performance during the split-sample tests. However, it became
437 apparent that the two MLR-based methods resulted in more closely simulation results than the SP-based approach.
438 This indicates that the method selection, such as spatial proximity-based or regression-based, has a greater influ-
439 ence on the regionalization than the details of executing the method. Moreover, the split-sample test should be



440 extended to get deeper insights into the method's robustness. For example, the SP and SI robustness check could
441 be extended by the so-called “HDes” approach, which Lebecherel et al. (2016) recommended. In this approach,
442 the closest basin to the corresponding (pseudo-) ungauged basin would be ignored during the regionalization to
443 measure the robustness of the regionalization method.

444 4. Conclusion

445 Valid simulation results from GHMs, such as WaterGAP3, are crucial for detecting hotspots or studying patterns
446 in climate change impacts. However, the lack of worldwide monitoring data makes adapting GHMs' parameters
447 for valid global simulations challenging. Therefore, regionalization is necessary to estimate parameters in un-
448 gauged basins. This study introduces novel regionalization methods for WaterGAP3 and aims to provide insights
449 into selecting a suitable regionalization method and evaluating its impact on the simulation results. Traditional and
450 machine learning-based methods are tested to assess the advantages of using new techniques on a global scale.
451 The concept of benchmark-to-beat and an ensemble of split-sampling tests are employed for a comprehensive
452 evaluation.

453 Our results suggest that the basin descriptor selection may not be crucial for regionalization in WaterGAP3 as long
454 as a subset of the selected descriptors contains relevant information. Additionally, introducing an ensemble ap-
455 proach for Similarity Indices does not necessarily improve the prediction performance but increases the likelihood
456 of robust predictions. Interestingly, the simplest regionalization method (using the concept of spatial proximity)
457 outperforms most of the developed regionalization methods and the benchmark-to-beat. In contrast, the more com-
458 plex, machine learning-based approaches deliver insufficient prediction performance. The inadequate performance
459 may be attributed to an inefficient extraction of available information content from the descriptors and the blurring
460 relationship between the calibration parameter and basin descriptors, which is caused by including multiple error
461 sources in the calibration parameter values. This blurring relationship probably poses a high risk of over-parame-
462 terization, which hinders the use of more flexible machine learning-based approaches.

463 Regionalization appears to result in spatially varying uncertainty for ungauged regions, with India and Indonesia
464 being particularly affected by higher uncertainty. The local impacts of regionalization in ungauged areas propagate
465 to the global scale, where the water balance component “outflow to the ocean and inland sinks” changed by about
466 $2400 \text{ km}^3 \text{ yr}^{-1}$, which is in the scale of inter-model differences. As the selected regionalization method influences
467 the regionalization more than details on the execution of the method, we recommend employing simulation runs
468 that use multiple regionalization methods to account for the uncertainty induced by the chosen regionalization
469 method. Considering the uncertainty induced by regionalization is especially important when analysing regions
470 with a significant proportion of ungauged basins or high sensitivity to the examined target.

471 *Code and data availability.* The data and the supporting R-Code to reproduce this study's findings are available at
472 DOI 10.5281/zenodo.10803089.

473 *Authors contribution.* JK developed, designed, and drafted the study. NK helped to design the experiment. MF
474 provided feedback throughout the entire process and supported the writing.

475 *Competing interests.* The authors declare that they have no conflict of interest.



476 **Appendix A: Basin descriptors**

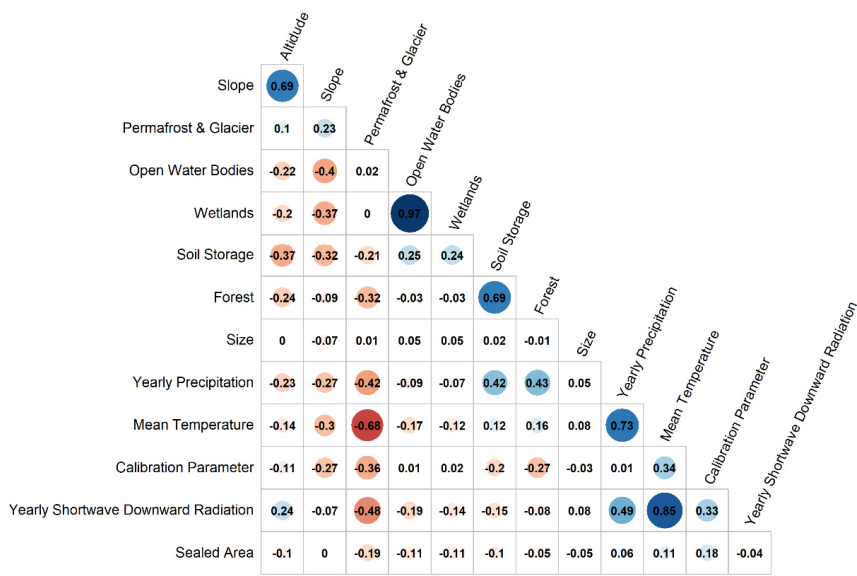
477 Overview of basins descriptors used in this study. All basin descriptors are derived from the original model input
478 and aggregated with a simple mean method to basin values to produce the same spatial resolution as the calibrated
479 model parameter.

- 480 • *Soil Storage*: The size of the soil storage, i.e., the maximal water content in the soil reachable for plants
481 in millimetres. The information is the product of rooting depth (defined in a look-up table) and the total
482 available water content derived from Batjes (2013).
- 483 • *Open Water Bodies*: The fraction of the area covered with open water bodies in the basin is given as a
484 percentage. The model input is based on the GLWD database (Lehner & Döll, 2004).
- 485 • *Wetlands*: The fraction of area covered with wetlands in a basin is given in percentage. The model input
486 is based on the GLWD database (Lehner & Döll, 2004).
- 487 • *Size*: Size of a basin in km²
- 488 • *Slope*: The mean slope class is calculated as described in Döll & Fiedler (2008) and based on GTOPO30
489 (USGS EROS data centre).
- 490 • *Altitude*: The mean altitude of a basin is given in metres above sea level and based on GTOPO30 (USGS
491 EROS data centre).
- 492 • *Forest*: The mean fraction of the area covered with forest is given in percentage and derived from MODIS
493 data (Friedl & Sulla-Menashe, 2019), where 2001 is used as a reference. All grid cells having a dominant
494 International Geosphere-Biosphere Programme (IGBP) classification between one and five are defined
495 as “forest”.
- 496 • *Sealed Area*: The mean fraction of sealed area is given in percentage and derived from MODIS data
497 (Friedl & Sulla-Menashe, 2019), where 2001 is used as a reference. All grid cells having an IGBP clas-
498 sification equal to 13 are defined as they would contain 60% of the sealed area. Note: The different treat-
499 ment of forest and sealed area is based on the required model input; whereas the land cover is a classified
500 value, the sealed area is a floating-point value.
- 501 • *Permafrost & Glacier*: The mean coverage of permafrost and glacier in a basin is given in percentage. It
502 is based on the World Glacier Inventory and the Circum-Arctic Map of Permafrost and Ground-Ice Con-
503 ditions.
- 504 • *Mean Temperature*: The mean air temperature is based on the meteorological forcing used to drive the
505 model (Lange, 2019) covering the period 1979 to 2016 and given in degrees Celsius.
- 506 • *Yearly Precipitation*: The yearly precipitation sum is based on the meteorological forcing used to drive
507 the model (Lange, 2019) covering the period 1979 to 2016 and given in millimetres.
- 508 • *Yearly Shortwave Downward Radiation*: The yearly shortwave downward radiation is based on the me-
509 teorological forcing used to drive the model (Lange, 2019) covering the period 1979 to 2016 and given
510 in Wm².

511

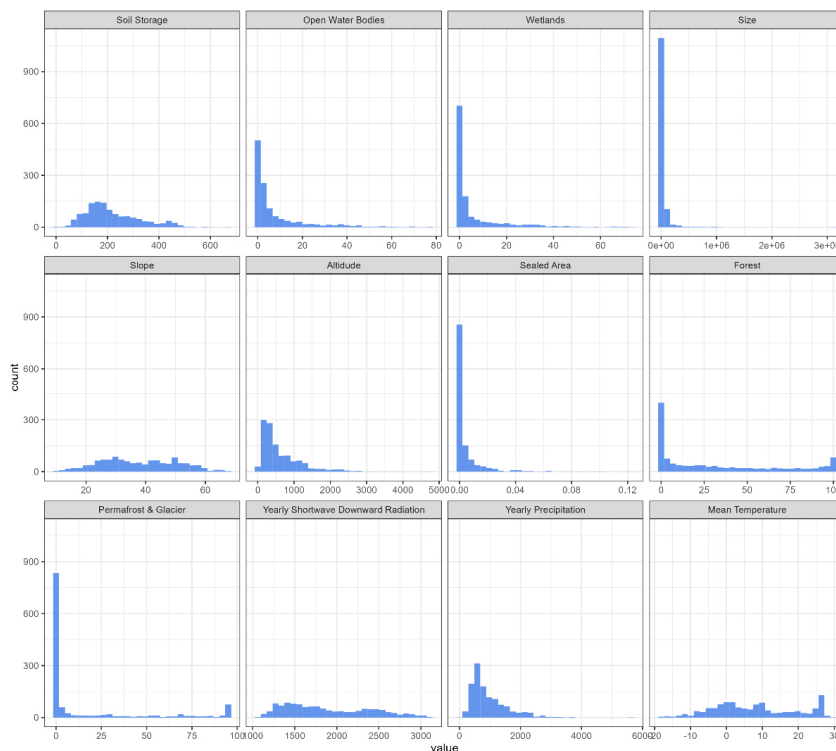
512 The correlation between the defined basin descriptors is shown in Fig. A1. The variation within each basin de-
513 scriptor for basins used for regionalization is shown in Fig. A2.

514



515
 516
 517

Figure A1: Correlation between basins descriptors.



518
 519

Figure A2: Distribution of basins descriptors within all basins used for regionalization (n=1,236)



520 **Appendix B: Results of split-sample tests**

521 **Table B1: Summarized results of the split-sample tests for all regionalization methods**

input	method	train (median)	train (sd)	test (median)	test (sd)
-	WG2	1.527	0.042	1.544	0.046
-	SP	-	-	1.356	0.057
cl	MLR	1.474	0.039	1.485	0.019
p		1.871	0.034	1.881	0.015
p+cl		1.457	0.038	1.473	0.018
all		1.394	0.039	1.425	0.024
cl	MLR_t	1.322	0.040	1.331	0.027
p		1.830	0.041	1.843	0.030
p+cl		1.307	0.042	1.337	0.030
all		1.245	0.042	1.292	0.034
cl	RF	0.688	0.026	1.401	0.029
p		0.741	0.027	1.579	0.032
p+cl		0.620	0.020	1.312	0.025
all		0.624	0.021	1.346	0.023
cl	RF_t	0.465	0.020	1.310	0.039
p		0.494	0.023	1.540	0.042
p+cl		0.378	0.017	1.183	0.037
all		0.345	0.014	1.181	0.034
cl	SI_1	1.477	0.080	1.492	0.056
p		1.651	0.086	1.661	0.063
p+cl		1.380	0.066	1.375	0.050
all		1.367	0.069	1.390	0.064
cl	SI_10	1.398	0.046	1.397	0.029
p		1.558	0.047	1.556	0.027
p+cl		1.326	0.044	1.321	0.025
all		1.398	0.049	1.402	0.028
cl	SI_10_t	1.281	0.053	1.281	0.043
p		1.497	0.050	1.487	0.037
p+cl		1.206	0.048	1.201	0.040
all		1.286	0.053	1.296	0.039
cl	k-means	1.689	0.038	1.699	0.018
p		1.910	0.051	1.918	0.039
p+cl		1.632	0.046	1.648	0.022
all		1.642	0.044	1.638	0.025
cl	k-means_t	1.474	0.111	1.519	0.088
p		1.909	0.055	1.918	0.040
p+cl		1.399	0.070	1.425	0.053
all		1.426	0.068	1.417	0.051
cl	k-means flexible	1.065	0.048	1.553	0.097
p		1.191	0.046	1.991	0.142
p+cl		0.982	0.040	1.568	0.125
all		0.957	0.044	1.515	0.114



522 **References**

- 523 Arheimer, B., Pimentel, R., Isberg, K., Crochemore, L., Andersson, J. C. M., Hasan, A., & Pineda, L.: Global
524 catchment modelling using World-Wide HYPE (WWH), open data, and stepwise parameter estimation, *Hydrology
525 and Earth System Sciences*, 24(2), 535–559. <https://doi.org/10.5194/hess-24-535-2020>, 2020.
- 526 Arsenault, R., & Brissette, F. P.: Continuous streamflow prediction in ungauged basins: The effects of equifinality
527 and parameter set selection on uncertainty in regionalization approaches, *Water Resources Research*, 50, 6135–
528 6153, <https://doi.org/10.1002/2013WR014898>, 2014.
- 529 Ayzel, G. V., Gusev, E. M., & Nasonova, O. N.: River runoff evaluation for ungauged watersheds by SWAP
530 model. 2. Application of methods of physiographic similarity and spatial geostatistics, *Water Resources*, 44(4),
531 547–558, <https://doi.org/10.1134/S0097807817040029>, 2017.
- 532 Barbarossa, V., Bosmans, J., Wanders, N., King, H., Bierkens, M. F. P., Huijbregts, M. A. J., & Schipper, A. M.:
533 Threats of global warming to the world's freshwater fishes, *Nature Communications*, 12(1), 1701,
534 <https://doi.org/10.1038/s41467-021-21655-w>, 2021.
- 535 Batjes, N. H.: ISRIC-WISE derived soil properties on a 5 by 5 arc-minutes global grid (ver. 1.2) [data set],
536 <https://data.isric.org/geonetwork/srv/eng/catalog.search#/metadata/82f3d6b0-a045-4fe2-b960-6d05bc1f37c0>,
537 2013.
- 538 Beck, H. E., Pan, M., Lin, P., Seibert, J., van Dijk, A. I. J. M., & Wood, E. F.: Global Fully Distributed Parameter
539 Regionalization Based on Observed Streamflow From 4,229 Headwater Catchments, *Journal of Geophysical Re-
540 search: Atmospheres*, 125(17), <https://doi.org/10.1029/2019JD031485>, 2020.
- 541 Beck, H. E., van Dijk, A. I. J. M., Roo, A. de, Dutra, E., Fink, G., Orth, R., & Schellekens, J.: Global evaluation of
542 runoff from 10 state-of-the-art hydrological models, *Hydrol. Earth Syst. Sci.*, 21, 2881–20903,
543 <https://doi.org/10.5194/hess-21-2881-2017>, 2017.
- 544 Beck, H. E., van Dijk, A. I. J. M., Roo, A. de, Miralles, D. G., McVicar, T. R., Schellekens, J., & Bruijnzeel, L.
545 A.: Global-scale regionalization of hydrologic model parameters, *Water Resources Research*, 52(5), 3599–3622,
546 <https://doi.org/10.1002/2015WR018247>, 2016.
- 547 Boulange, J., Hanasaki, N., Yamazaki, D., & Pokhrel, Y.: Role of dams in reducing global flood exposure under
548 climate change, *Nature Communications*, 12(1), 417, <https://doi.org/10.1038/s41467-020-20704-0>, 2021.
- 549 Breimann, L.: Random Forests, *Machine Learning*, 45, 1–32, <https://doi.org/10.1023/A:1010933404324>, 2001.
- 550 Chaney, N. W., Herman, J. D., Ek, M. B., & Wood, E. F.: Deriving global parameter estimates for the Noah land
551 surface model using FLUXNET and machine learning, *Journal of Geophysical Research: Atmospheres*, 121(22),
552 13,218–13,235, <https://doi.org/10.1002/2016JD024821>, 2016.
- 553 Cuntz, M., Mai, J., Samaniego, L., Clark, M., Wulfmeyer, V., Branch, O., Attinger, S., & Thober, S.: The impact
554 of standard and hard-coded parameters on the hydrologic fluxes in the Noah-MP land surface model, *Journal of
555 Geophysical Research: Atmospheres*, 121, 10,676 - 10,700, <https://doi.org/10.1002/2016JD025097>, 2016.
- 556 Döll, P. & Fiedler, K.: Global-scale modeling of groundwater recharge, *Hydrol. Earth Syst. Sci.*, 12, 863–885,
557 <https://doi.org/10.5194/hess-12-863-2008>, 2008



- 558 Döll, P., Kaspar, F., & Lehner, B.: A global hydrological model for deriving water availability indicators: model
559 tuning and validation, *Journal of Hydrology*, 270, 105–13, [https://doi.org/10.1016/S0022-1694\(02\)00283-4](https://doi.org/10.1016/S0022-1694(02)00283-4), 2003.
- 560 Eisner, S.: Comprehensive Evaluation of the WaterGAP3 Model across Climatic, Physiographic, and Anthropo-
561 genic Gradients, PhD thesis, University of Kassel, Kassel, Germany, 128pp., 2016.
- 562 Friedl, M., Sulla-Menashe, D.: MCD12Q1 MODIS/Terra+Aqua Land, Cover Type Yearly L3 Global 500m SIN
563 Grid V006 [data set], NASA EOSDIS Land Processes DAAC, <https://doi.org/10.5067/MODIS/MCD12Q1.006>,
564 2019.
- 565 Feigl, M., Thober, S., Schweppe, R., Herrnegger, M., Samaniego, L., & Schulz, K.: Automatic Regionalization of
566 Model Parameters for Hydrological Models, *Water Resources Research*, 58, e2022WR031966,
567 <https://doi.org/10.1029/2022WR031966>, 2022.
- 568 Golian, S., Murphy, C., & Meresa, H.: Regionalization of hydrological models for flow estimation in ungauged
569 catchments in Ireland, *Journal of Hydrology: Regional Studies*, 36, 100859,
570 <https://doi.org/10.1016/j.ejrh.2021.100859>, 2021.
- 571 GRDC, The Global Runoff Data Centre, 56068 Koblenz, Germany, 2020.
- 572 Guo Y, Zhang Y, Zhang L, & Wang Z: Regionalization of hydrological modeling for predicting streamflow in
573 ungauged catchments: A comprehensive review, *WIREs Water*, 8, e1487, <https://doi.org/10.1002/wat2.1487>, 2021
- 574 Gupta, H. V, Sorooshian, S., & Yapo, P. O.: Toward improved calibration of hydrologic models: Multiple and
575 noncommensurable measures of information, *Water Resources Research*, 34(4), 751–763,
576 <https://doi.org/10.1029/97WR03495>, 1998.
- 577 He, Y., Bárdossy, A., & Zehe, E.: A review of regionalisation for continuous streamflow simulation, *Hydrology
578 and Earth System Sciences*, 15(11), 3539–3553. <https://doi.org/10.5194/hess-15-3539-2011>, 2011.
- 579 Kaspar, F.: Entwicklung und Unsicherheitsanalyse eines globalen hydrologischen Modells, PhD thesis, University
580 of Kassel, Kassel, Germany, 129pp., 2004.
- 581 Krabbenhoft, C. A., Allen, G. H., Lin, P., Godsey, S. E., Allen, D. C., Burrows, R. M., DelVecchia, A. G., Fritz,
582 K. M., Shanfield, M., Burgin, A. J., Zimmer, M. A., Detry, T., Dodds, W. K., Jones, C. N., Mims, M. C., Franklin,
583 C., Hammond, J. C., Zipper, S., Ward, A. S., Olden, J. D.: Assessing placement bias of the global river gauge
584 network, *Nature Sustainability*, 5, 586–592. <https://doi.org/10.1038/s41893-022-00873-0>, 2022.
- 585 Kupzig, J., Reinecke, R., Pianosi, F., Flörke, M., & Wagener, T.: Towards parameter estimation in global hydro-
586 logical models, *Environmental Research Letters*, 18(7), 74023. <https://doi.org/10.1088/1748-9326/acdae8>, 2023.
- 587 Lange, S.: Earth2Observe, WFDEI and ERA-Interim data Merged and Bias-corrected for ISIMIP (EWEMBI), V.
588 1.1 [data set], GFZ Data Services, <https://doi.org/10.5880/pik.2019.004>, 2019.
- 589 Lebecherel, L., Andréassian, V., Perrin: On evaluating the robustness of spatial-proximity-based regionalization
590 methods, *Journal of Hydrology*, 539, 196–203, <https://doi.org/10.1016/j.jhydrol.2016.05.031>, 2016.
- 591 Lehner, B. and Döll, P.: Development and validation of a global database of lakes, reservoirs and wetlands, *Journal
592 of Hydrology*, 296 (1-4), 1-22, <https://doi.org/10.1016/j.jhydrol.2004.03.028>, 2004.



- 593 Lehner, B., Verdin, K., & Jarvis, A.: New global hydrography derived from spaceborne elevation data, *Eos, Trans-*
594 *actions, AGU*, 89, 93–94, doi:10.1029/2008EO100001, 2008.
- 595 Liam, A., & Wiener, M.: Classification and Regression by randomForest. *R News*, 2(3), 18–22, 2002.
- 596 Lindström, G., Johansson, B., Persson, M., Gardelin, M., & Bergström, S.: Development and test of the distributed
597 HBV-96 hydrological model, *Journal of Hydrology*, 201, 272–288, <https://doi.org/10.1016/S0022->
598 [1694\(97\)00041-3](https://doi.org/10.1016/S0022-1694(97)00041-3), 1997.
- 599 McIntyre, N, Lee, H., Wheater, H., Young, A., & Wagener, T.: Ensemble predictions of runoff in ungauged catch-
600 ments, *Water Resources Research*, 41(12), W12434, <https://doi.org/10.1029/2005WR004289>, 2005.
- 601 Müller Schmied, H., Cáceres, D., Eisner, S., Flörke, M., Herbert, C., Niemann, C., Peiris, T. A., Popat, E., Port-
602 mann, F. T., Reinecke, R., Schumacher, M., Shadkam, S., Telteu, C.-E., Trautmann, T., & Döll, P.: The global
603 water resources and use model WaterGAP v2.2d: model description and evaluation, *Geoscientific Model Devel-*
604 *opment*, 14(2), 1037–1079, <https://doi.org/10.5194/gmd-14-1037-2021>, 2021.
- 605 Nijssen, B., O'Donnell, G. M., Lettenmeier, D. P., Lohmann, D., & Wood, E. F.: Predicting the Discharge of
606 Global Rivers, *American Meteorological Society*, 3307–3323, <https://doi.org/10.1175/1520->
607 [0442\(2001\)014<3307:PTDOGR>2.0.CO;2](https://doi.org/10.1175/1520-0442(2001)014<3307:PTDOGR>2.0.CO;2), 2000.
- 608 Oudin, L., Andréassian, V., Perrin, C., Michel, C., & Le Moine, N.: Spatial proximity, physical similarity, regres-
609 sion and ungauged catchments: A comparison of regionalization approaches based on 913 French catchments, *Wa-*
610 *ter Resources Research*, 44(3), W03413, <https://doi.org/10.1029/2007WR006240>, 2008.
- 611 Oudin, L., Kay, A., Andréassian, V., & Perrin, C.: Are seemingly physically similar catchments truly hydrologi-
612 cally similar? *Water Resources Research*, 46(11), W11558, <https://doi.org/10.1029/2009WR008887>, 2010.
- 613 Pagliero, L., Bouraoui, F., Diels, J., Willems, P., & McIntyre, N.: Investigating regionalization techniques for
614 large-scale hydrological modelling, *Journal of Hydrology*, 570, 220–235, <https://doi.org/10.1016/j.jhy->
615 [drol.2018.12.071](https://doi.org/10.1016/j.jhydrol.2018.12.071), 2019.
- 616 Parajka, J., Merz, R., & Blöschl, G.: A comparison of regionalisation methods for catchment model parameters,
617 *Hydrology and Earth System Sciences*, 9, 157–171, <https://doi.org/10.5194/hess-9-157-2005>, 2005.
- 618 Parajka, J., Viglione, A., Rogger, M., Salinas, J. L., Sivaplan, M. & Blöschl, G.: Comparative assessment of pre-
619 diction in ungauged basins – Part 1: Runoff-hydrograph studies, *Hydrology and Earth System Sciences*, 17, 1783-
620 1795, www.hydrol-earth-syst-sci.net/17/1783/2013/, 2013.
- 621 Poissant, D., Arsenault, R. & Brissette, F.: Impact of parameter set dimensionality and calibration procedures on
622 streamflow prediction at ungauged catchments, *Journal of Hydrology: Regional Studies*, 12, 220–237,
623 <https://doi.org/10.1016/j.ejrh.2017.05.005>, 2017.
- 624 Pool, S., Vis, M., & Seibert, J.: Regionalization for ungauged catchments — Lessons learned from a comparative
625 large-sample study. *Water Resources Research*, 57, e2021WR030437. <https://doi.org/10.1029/2021WR030437>,
626 2021.



- 627 Qi, W., Chen, J., Li, L., Xu, C., Li, J., Xiang, Y., & Zhang, S.: A framework to regionalize conceptual model
628 parameters for global hydrological modelling, *Hydrology and Earth System Sciences Discussions* [preprint],
629 <https://doi.org/10.5194/hess-2020-127>, 2020.
- 630 R Core Team.: R: A language and environment for statistical computing R Foundation for Statistical Computing,
631 Vienna, Austria. <https://www.r-project.org/>, 2020.
- 632 Reichl, J. P. C., Western, A. W., McIntyre, N. R. & Chiew, F. H. S: Optimization of a Similarity Measure for
633 Estimating Ungauged Streamflow, *Water Resources Research*, 45 (10), <https://doi.org/10.1029/2008WR007248>,
634 2009
- 635 Samaniego, L., Kumar, R & Attinger, S.: Multiscale parameter regionalization of a grid-based hydrologic model
636 at the mesoscale, *Water Resources Research*, 46(5), W05523, <https://doi.org/10.1029/2008WR007327>, 2010.
- 637 Schaeffli, B., & Gupta, H. V.: Do Nash values have value?, *Hydrological Processes*, 21(15), 2075–2080,
638 <https://doi.org/10.1002/hyp.6825>, 2007.
- 639 Schweppe, R., Thober, S., Müller, S., Kelbling, M., Kumar, R., Attinger, S., & Samaniego, L.: MPR 1.0: a stand-
640 alone multiscale parameter regionalization tool for improved parameter estimation of land surface models, *Geo-*
641 *scientific Model Development*, 15, 859–882, <https://doi.org/10.5194/gmd-15-859-2022>, 2022.
- 642 Seibert, J.: On the need for benchmarks in hydrological modelling, *Hydrological Processes*, 15(6), 1063–1064,
643 <https://doi.org/10.1002/hyp.446>, 2001.
- 644 Shannon, C. E.: A Mathematical Theory of Communication, *The Bell System Technical Journal*, 3(27), 379–423,
645 <https://doi.org/10.1002/j.1538-7305.1948.tb01338.x>, 1948.
- 646 Stacke, T., & Hagemann, S.: HydroPy (v1.0): a new global hydrological model written in Python, *Geoscientific*
647 *Model Development*, 14, 7795–7816, <https://doi.org/10.5194/gmd-14-7795-2021>, 2021.
- 648 Tang, Y., Marshall, L., Sharma, A. & Smith, T.: Tools for investigating the prior distribution in Bayesian hydrology,
649 *Journal of Hydrology*, 538, 551–562, <https://doi.org/10.1016/j.jhydrol.2016.04.032>, 2016.
- 650 Tongal, H., & Sivakumar, B.: Cross-entropy clustering framework for catchment classification, *Journal of Hydrology*,
651 552, 433–446, <https://doi.org/10.1016/j.jhydrol.2017.07.005>, 2017.
- 652 Venables, W. N., & Ripley, B. D.: *Modern Applied Statistics with S* (Fourth Edition). Springer Science+Business
653 Media New York, USA, 501pp, ISBN 978-1-4419-3008-8, 2002
- 654 Wagener, T., Wheeler, H. S., & Gupta, H. V. (2004). *Rainfall – Runoff Modelling in Gauged and Ungauged*
655 *Catchments*, Imperial College Press, London, UK, 332pp., <https://doi.org/10.1142/p335>, 2004.
- 656 Widén-Nilsson, E., Halldin, S., & Xu, C.: Global water-balance modelling with WASMOD-M: Parameter estimation
657 and regionalisation, *Journal of Hydrology*, 340(1-2), 105–118, <https://doi.org/10.1016/j.jhydrol.2007.04.002>,
658 2007.
- 659 Wu, H., Zhang, J., Bao, Z., Wang, G., Wang, W., Yang, Y. & Wang, J.: Runoff Modeling in Ungauged Catchments
660 Using Machine Learning Algorithm-Based Model Parameters Regionalization Methodology, *Engineering*, 28, 93–
661 104, <https://doi.org/10.1016/j.eng.2021.12.014>, 2023.



- 662 Yang, X., Magnusson, J., Huang, S., Beldring, S., & Xu, C.: Dependence of regionalization methods on the com-
663 plexity of hydrological models in multiple climatic regions, *Journal of Hydrology*, 582, 124357,
664 <https://doi.org/10.1016/j.jhydrol.2019.124357>, 2020.
- 665 Yoshida, T., Hanasaki, N., Nishina, K., Boulange, J, Okada, M., & Troch, P. A.: Inference of Parameters for a
666 Global Hydrological Model: Identifiability and Predictive Uncertainties of Climate-Based Parameters, *Water Re-
667 sources Research*, 58, e2021WR030666, <https://doi.org/10.1029/2021WR030660>, 2022.